ACCOUNTS
of chemical research

Controlled Plasmonic Nanostructures for Surface-Enhanced Spectroscopy and Sensing

JON P. CAMDEN, JON A. DIERINGER, JING ZHAO, AND RICHARD P. VAN DUYNE*

Department of Chemistry, Northwestern University, 2145 Sheridan Road, Evanston, Illinois 60208

RECEIVED ON FEBRUARY 4, 2008

CONSPECTUS

After its discovery more than 30 years ago, surface-enhanced Raman spectroscopy (SERS) was expected to have major impact as a sensitive analytical technique and tool for fundamental studies of surface species. Unfortunately, the lack of reliable and reproducible fabrication methods limited its applicability. In recent years, SERS has enjoyed a renaissance, and there is renewed interest in both the fundamentals and applications of SERS. New techniques for nanofabrication, the design of substrates that maximize the electromagnetic enhancement, and the discovery of single-molecule SERS are driving the resurgence of this field.

This Account highlights our group's recent work on SERS. Initially, we discuss SERS substrates that have shown proven reproducibility, stability, and large field enhancement. These substrates enable many analytical applications, such as anthrax detection, chemical warfare agent stimulant detection, and in vitro and in vivo glucose sensing. We then turn to a detailed study of the wavelength and distance dependence of SERS, which further illustrate predictions obtained from the electromagnetic enhancement mechanism. Last, an isotopic labeling technique applied to the rhodamine 6G (R6G)/silver system serves as an additional proof of the existence of single-molecule SERS and explores the dynamical features of this process. This work, in conjunction with theoretical calculations, allows us to comment on the possible role of charge transfer in the R6G/silver system.

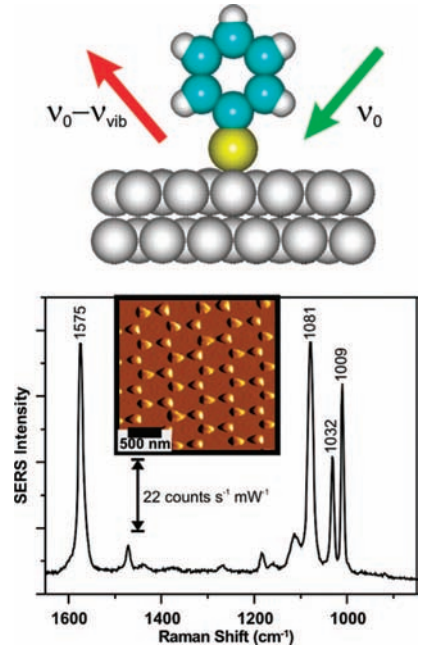

I. Introduction

In 1977, Jeanmaire and Van Duyne[1] and Albrecht and Creighton[2] independently observed that adsorption of pyridine to electrochemically roughened silver surfaces could increase the pyridine Raman scattering intensity by a factor of $\sim 10^6$. This striking discovery was denoted the surface-enhanced Raman scattering (SERS) effect and immediately became the subject of intensive study. The widespread application of SERS to problems of chemical interest, however, was limited by obstacles such as the irreproducibility of substrates and controversy over the nature of the large enhancements. Recently there has been a renewed interest in SERS as exciting advances of the past 10−15 years have overcome many of the previous difficulties. We cite three main achievements as drivers of this current renaissance: (1) the application of nanofabrication techniques to reproducibly manufacture well-defined substrates with nanometer scale features, (2) the design of substrates that maximize the EM enhancement, and (3) the discovery of single-molecule SERS (SMSERS).[3,4]

Our current understanding of the SERS effect is due to a large number of researchers working over the last several decades; for example, see

Published on the Web 07/17/2008
10.1021/ar800041s CCC: $40.75

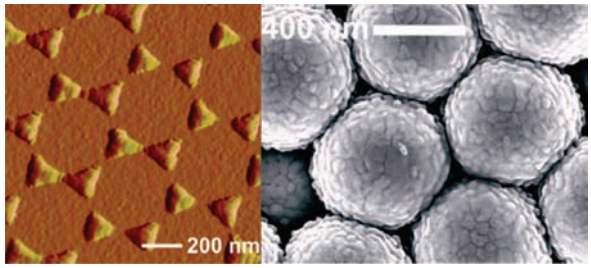

FIGURE 1. Images of NSL-fabricated nanostructures: left, AFM image of Ag nanotriangle arrays; right, SEM images of a AgFON surface.

historical perspectives by Van Duyne[5] and Moskovits,[6] as well as review articles.[7−10] In this Account, however, we focus on work from our laboratory, beginning with a discussion of substrates that provide large SERS enhancements as well as exhibiting reproducibility and stability. Then, we present experimental evidence for the postulated wavelength and distance dependence of the EM mechanism of SERS. Next, we offer a frequency domain proof of SMSERS behavior using isotopically labeled rhodamine 6G (R6G) and discuss enhancement factors in SMSERS. Last, we briefly explore the possible role of charge transfer in the R6G/silver system.

II. Fundamental Studies of the SERS Effect

A. Substrates Fabricated by Nanosphere Lithography (NSL). Nanosphere lithography (NSL), developed by Van Duyne and co-workers,[11,12] provides a method to fabricate nanoparticle arrays with a tunable localized surface plasmon resonance (LSPR). In this technique, nanospheres are self-assembled into a monolayer or bilayer on the substrate. Metal is then deposited through the nanosphere mask, and after removal of the nanospheres, a periodic array of metal nanostructures remains on the substrate. Figure 1 shows the AFM image of the resulting nanoparticle array. The size and spacing of the nanostructures and consequently the position of the LSPR of NSL-fabricated nanostructures can be controlled by the nanosphere size and deposited metal thickness. It has been demonstrated both experimentally and theoretically that the sharp tips of the NSL nanotriangles give rise to EM enhancement factors as large as 10^8.[13−15] The most typical nanostructures fabricated by NSL are triangular nanoparticle arrays; however, a wide range of other nanostructres can be fabricated.[11]

If the sphere mask is not removed after metal deposition, then the metal film-over-nanospheres (FON) substrate is obtained. Figure 1 shows the SEM image of the FON surface. FON substrates have broader LSPR resonances compared with NSL nanoprism arrays; however, they provide a large surface area available for binding and detection.[16] Functionalization of FON substrates is a crucial feature of sensing experiments and these modified surfaces have been used for in vitro[17−19] and in vivo[20] glucose sensing and anthrax biomarker detection.[21,22]

SERS activity is affected by the oxidation of the metal, the lack of stability of the nanostructures when exposed to buffer solutions, and annealing at high temperatures. There are several methods to mitigate these unwanted effects. For example, we have combined NSL and reactive ion etching techniques to fabricate Ag nanoparticle arrays embedded in glass, which exhibit improved stability against mechanical force and solution flow.[23] In addition, adding an alumina overlayer by atomic layer deposition (ALD) to NSL-fabricated particles dramatically increases their thermal stability,[24] thus enabling SERS to be extended to high-temperature studies such as those important in heterogeneous catalysis. It is also known that alumina-coated AgFON silver film over nanospheres surfaces maintain their SERS activity under ambient conditions and avoid oxidation.[22] These surfaces have demonstrated anthrax biomarker detection with 12-month temporal stability.[25]

B. Wavelength Dependence of Surface-Enhanced Raman Spectroscopy. The EM mechanism of SERS[26−29] predicts that the EM enhancement factor E_{EM} is given by

$$E_{EM} = [g(\omega)]^2[g(\omega\prime)]^2 \quad (1)$$

In this expression ω is the incident laser frequency, ω' is the Stokes-shifted frequency of the Raman scattered photon, and g is the amount the local electric field at the molecule (E_{mol}) is enhanced relative to the far-field value of the electric field (E_0) and is given by $E_{mol} = gE_0$. Note that g is frequency dependent and that this local electric field enhancment experienced by the molecule results from the excitation of the localized surface plasmon resonance in the metal nanoparticle. According to eq 1, the maximum enhancement of the normal Raman cross-section occurs when both the incident and Stokes scattered fields are equally enhanced. Therefore, one should take care to choose the proper laser excitation frequency such that this frequency and the Raman Stokes-shifted frequency straddle the maximum extinction of the LSPR. As such, the frequency of laser excitation should be one-half of the Raman shift higher in energy than the LSPR spectral maximum. A consequence of this is that not all vibrational modes are optimally excited in a given spectrum. Although experiments were proposed at the inception of SERS to measure this effect, studies performed were inconclusive due to limitations in instrumentation and poor definition of the SERS substrates.[30−32] The ideal experiment is to have a continu-

ously tunable excitation and detection scheme over the bandwidth of a well-defined LSPR.

A systematic study of the optimum excitation wavelength as a function of the spectral position of the LSPR extinction was recently completed.[15] This was made possible by recent advances in nanofabrication allowing the production of substrates with well-defined and tunable LSPR resonances and better tunability in both the SERS excitation and detection. Figure 2 shows characteristic wavelength-scanned excitation profiles of three vibrational modes of benzenethiol: 1009, 1081, and 1575 cm^{-1}. The excitation profiles show that the highest SERS EF is observed when the excitation wavelength is higher in energy than the spectral maximum of the LSPR extinction spectrum. Gaussian fits were made to the profiles, and the distance in energy of the maximum of the excitation profile and the LSPR extinction spectrum is on the order of half of the vibrational energy and increasing with the magnitude of the Raman Stokes shift.

The experiment was also performed on multiple silver nanoparticle sizes and shapes with extinction spectra at various locations in the visible region of the electromagnetic spectrum. In all cases, the magnitude of the energy separation between the excitation profile maximum and the LSPR extinction maximum is roughly half. An analogous experiment can also be performed by varying the spectral location of the LSPR relative to a fixed frequency laser, and similar results are observed.[13] Consequently, in order to achieve maximum EM enhancement, one should either prepare the sample such that the LSPR extinction is in the proper location for fixed laser frequency apparatus or set the wavelength to a higher frequency than the LSPR extinction in tunable systems. In the wavelength-scanned experiment, the relevant LSPR extinction spectrum is the one observed after adsorption of the analyte because the LSPR extinction spectrum is sensitive to the dielectric environment. These experiments illustrate the importance of optimizing the plasmon and excitation wavelengths to achieve maximum SERS EFs. We further conclude that both the incident and scattered photons in SERS are indeed enhanced.

C. Distance Dependence of Surface-Enhanced Raman Spectroscopy. One important consequence of the EM mechanism of SERS is that the adsorbate is not required to be in direct contact with the surface. This results because the enhanced electric fields extend beyond the surface creating a sensing volume within a few nanometers of the surface. The ability to enhance Raman scattering from molecules not directly attached to the surface is of great importance for systems such as surface-immobilized biological molecules,[33]

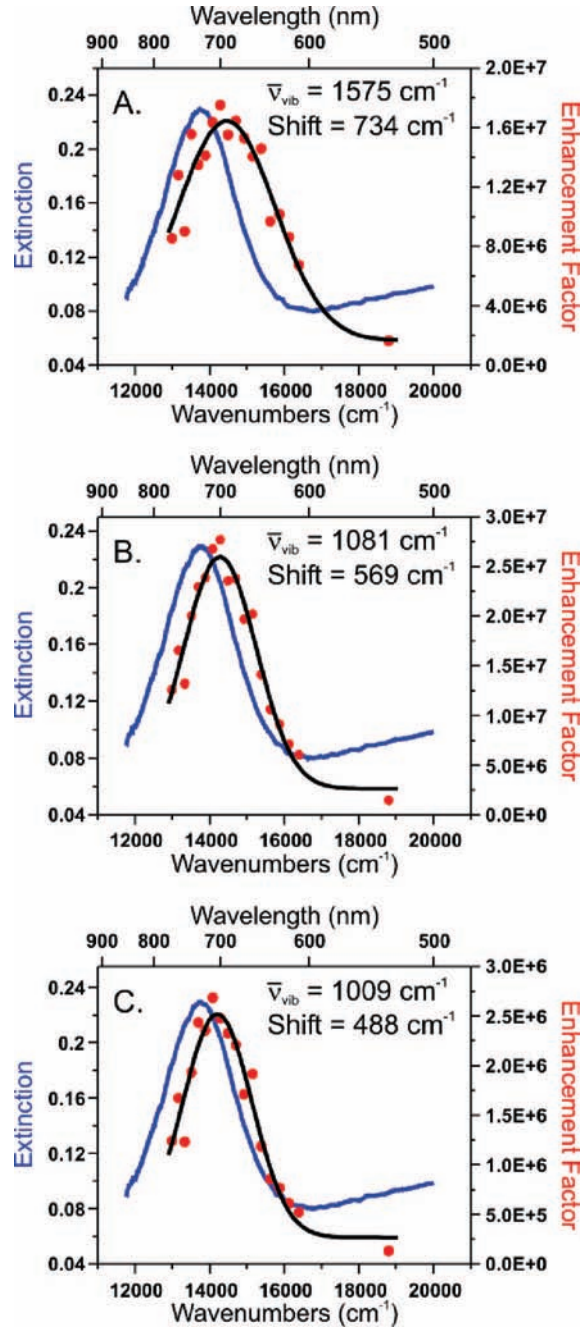

FIGURE 2. Three surface-enhanced Raman excitation profiles illustrating the effect of Stokes Raman shift: (A) profile of the 1575 cm^{-1} vibrational mode of benzenethiol—distance between LSPR λ_{max} and excitation profile fit line $\lambda_{ex,max}$ = 734 cm^{-1}; EF = 1.8 × 10^7; (B) 1081 cm^{-1} vibrational mode, shift = 569 cm^{-1}, EF = 2.8 × 10^7; (C) 1009 cm^{-1} vibrational mode, shift = 488 cm^{-1}, EF = 2.7 × 10^6. Reproduced with permission from ref 15. Copyright 2005 American Chemical Society.

where direct contact between the adsorbate of interest and the surface is not possible because the surface is modified with a capture layer for specificity or biocompatibility.

It has been shown that the SERS intensity of a given Raman mode, I_{SERS}, is a function of distance from the surface

$$I_{SERS} = \left(\frac{a+r}{a}\right)^{-10} \quad (2)$$

where a is the average size of the field-enhancing features on the surface.[34] This dependence on distance is a result of the r^{-3} decay of the field enhancement away from the surface, the 4th power dependence of I_{SERS} on the field enhancement, and the increased surface area scaling with r^2 as one considers shells of molecules at an increased distance from the nanoparticle.

The ideal distance-dependence experiment is one in which the thickness of the spacer layer could be easily varied in thickness from a few angstroms to tens of nanometers. Furthermore, the spacers would be conformal to handle roughened and nanostructured surfaces, pinhole free, and chemically uniform. We have deposited Al_2O_3 multilayers using ALD onto Ag film over nanosphere (AgFON) surfaces to probe the distance dependence of SERS.[35] Figure 3a shows the SER spectra for pyridine adsorbed on AgFON surfaces coated with four different thicknesses of ALD-deposited Al_2O_3. Figure 3b shows a plot of the relative intensity of the 1594 cm^{-1} band as a function of Al_2O_3 thickness. Fitting the experimental data to eq 2 leads to the average size of the enhancing particle, a = 12.0 nm. The term d_{10} defines the surface-to-molecule distance required to decrease the SERS intensity by a factor of 10. The data presented in this work clearly show that SERS is a long-range effect with a d_{10} value for this particular surface nanostructure of 2.8 nm. This value was derived assuming that a complete monolayer of Al_2O_3 was formed with each ALD cycle. Quartz crystal microbalance measurements have later shown that the average thickness of the ALD sequence is 1.1 Å and consequently a complete layer of alumina is not formed with each cycle. The mechanism for the formation of alumina on silver is still debated, but assuming that the quartz crystal microbalance measurements accurately model the initial growth of Al_2O_3 on silver, the measured value of d_{10} could be as low as 1 nm.[35]

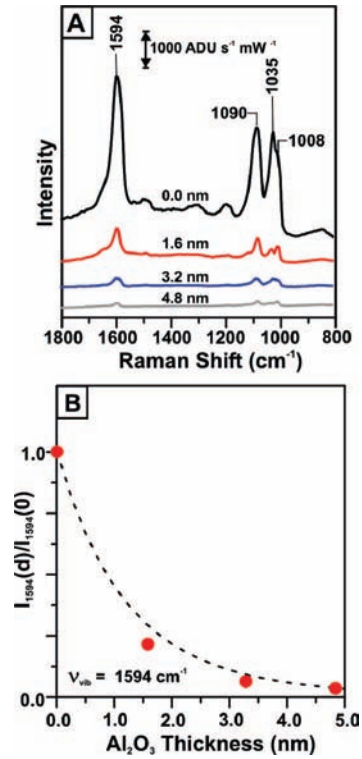

FIGURE 3. (A) SER spectra of pyridine adsorbed to silver film over nanosphere (AgFON) samples treated with various thicknesses of alumina (0.0, 1.6, 3.2, or 4.8 nm), ex = 532 nm, P = 1.0 mW, and acquisition time = 300 s and (B) plot of SERS intensity as a function of alumina thickness for the 1594 cm^{-1} band (filled circles). The solid curved line is a fit of this data to eq 2.[35] Reproduced by permission of The Royal Society of Chemistry (RSC).

III. Single-Molecule Surface-Enhanced Raman Scattering (SMSERS)

A.. Introduction and the Isotopologue Approach. SMSERS was independently reported in 1997 by Nie and Emory[3] and Kneipp et al.[4] Nie and Emory cited several features of their results that suggest single-molecule behavior: (1) Raman scattering is observed from single nanoparticles for analyte concentrations of less than 10^{-10} M, where each particle is expected to contain mostly zero or one analyte molecule, (2) unlike bulk SERS spectra, the observed single-molecule spectra show sensitivity to polarization, and (3) the position and intensity of vibrational bands exhibit sudden changes as a function of time. The work of Kneipp and co-workers[4,36] presented alternative evidence contingent on fluctuations in the intensity domain, using statistical analysis to support the claim of single-molecule behavior. Andersen et al.,[37] however, have shown that temporal fluctuation in peak intensity is not adequate evidence of SMSERS. Additionally, Pettinger and co-workers[38] point out that the SMSERS EF is strongly dependent on the molecule's position in the hot spot, and the variations would make the observation of quantized intensity impossible. Etchegoin et al.,[39] in their work examining the role of Poisson statistics in SMSERS, however, show that arguments based on Poisson statistics should not be regarded as sufficient proof for SMSERS behavior.

Despite the controversy over the use of Poisson statistics, there is other evidence that suggests SMSERS was observed, including (1) changes in the spectrum of an immobilized, isolated nanoparticle or nanoaggregate, for example, blinking or spectral wandering, (2) dependence of an isolated system on excitation power and polarization, and (3) observation of com-

peting analytes. Doering and Nie[40] concluded that blinking in SMSERS is due to surface diffusion in the proximity of a region of large EM enhancement, often called a hot spot, as evidenced by spectral interchange between R6G and the citrate background.

While the idea of electromagnetic hot spots in SERS is well-known,[27,28] Brus and co-workers[41,42] showed using polarization studies that hot spots formed at the junction of two nanoparticles likely play a major role in SMSERS, which was further supported by atomic force microscopy showing that SMSERS active structures are aggregates of Ag nanoparticles. In addition, SMSERS was shown to depend nonlinearly on excitation power, unlike SERS, which is ensemble averaged.[42] Le Ru and Etchegoin suggested a competing adsorbate approach using two different analytes (e.g., R6G and benzotriazole) to verify single-molecule behavior.[43,44] The application of this technique, which uses adsorbates with different chemical structure, however, is complicated due to differences in Raman cross section, absorption spectra, and surface binding affinity for the different analytes used. Similar considerations hold for two other reports using the competing adsorbate approach.[45,46] Pettinger and co-workers[38] have reiterated the point that Raman cross-sectional differences and variations in the surface chemistries for the two different adsorbates must be taken into account.

Our work in this field builds upon the competing adsorbate approach while circumventing its problematic issues. Two isotopologues of rhodamine 6G, R6G-d_0 and R6G-d_4, are used to demonstrate single-molecule character in the SER spectra. The use of two isotopologues (chemical species that differ only in the isotopic composition of their atoms) provides a method for performing dual-analyte SMSERS studies where the electronic absorption spectrum of the adsorbate is not perturbed, the surface chemistry remains unchanged, and the overall Raman cross section is similar. However, the vibrational bands having contributions from C−D stretching and bending will change in intensity and frequency, allowing the two isotopologues to be spectrally resolved. The frequency domain approach using two isotopologues of R6G permits single-molecule behavior to be verified by tracking the spectral signature of the individual species. When sufficiently low concentrations of both analyte molecules are introduced to a solution of silver nanoparticles such that, on average, only one type of molecule is adsorbed to each nanoparticle, each SMSER spectrum contains spectral features of only a single isotopologue.

B. A Frequency Domain Existence Proof of Single-Molecule Surface-Enhanced Raman Spectroscopy. The SER spectra from 50 individual nanoparticle aggregates were acquired, and only sites that were active were interrogated randomly. Figure 4a shows representative spectra from two of the spots measured, in which it is evident that there is only one isotopologue present in each probe volume. A histogram of occurrences of the three possible cases is given in Figure 4b. The observation that single isotopologue events dominate the sampling is strong evidence for SMSERS. Additionally, spectral wandering was observed in the 600 cm^{-1} range of the spectra. The degree of the spectral wandering observed is measured by a fit to the histograms of peak center frequency as seen in Figure 4c. The full width at half-maximum (fwhm) of the R6G-d_4 Gaussian fit and R6G-d_0 Gaussian fit were 3.0 and 4.8 cm^{-1}, respectively. As a control, the normal Raman scattering of the 1028.3 cm^{-1} mode of cyclohexane was collected to illustrate the instrumentation stability. The fwhm of the Gaussian fit for this mode's spectral fluctuation was 0.6 cm^{-1}. The fwhm of the ensemble-averaged spectra were 5.3 cm^{-1} for R6G-d_4 and 6.9 cm^{-1} for R6G-d_0. The single-molecule results indicate that the ensemble-averaged spectrum is a superposition of the single-molecule states. This analysis reveals the distribution of vibrational frequencies hidden under the ensemble average.

C. Surface Dynamics in Single-Molecule Surface-Enhanced Raman Spectroscopy. When the R6G/Ag system was under ambient environmental conditions (namely, humid laboratory air) at higher concentrations of molecules per nanoparticle, dynamic behavior or "blinking" was observed. Statistically, ca. 50 R6G-d_0 and 50 R6G-d_4 molecules were adsorbed per nanoparticle. Figure 5a shows a waterfall plot of inelastic scattering as a function of time. At $t = 0$ s, the spectrum appears to have only R6G-d_0 character, which is surprising considering the high dye concentration on the surface. The integrated intensity is on the same order of magnitude as the static, low-concentration experiment above, indicating that only a single molecule is scattering and not the 100 in the ensemble. Therefore, the EF in the hot spot must be at least 3−4 orders of magnitude greater than the average SERS EF of the nanoparticle, in agreement with previously published results.[3,48] As time progresses, the spectrum changes completely from R6G-d_0 to R6G-d_4 and back to R6G-d_0 over the course of 1000 s as displayed in Figure 5b.

There are two interpretations of the switching behavior considering that the SMSERS aggregates contain multiple potential hot spots: (1) two or more molecules are competing for the same hot spot on the nanoparticle surface, or (2) two or more

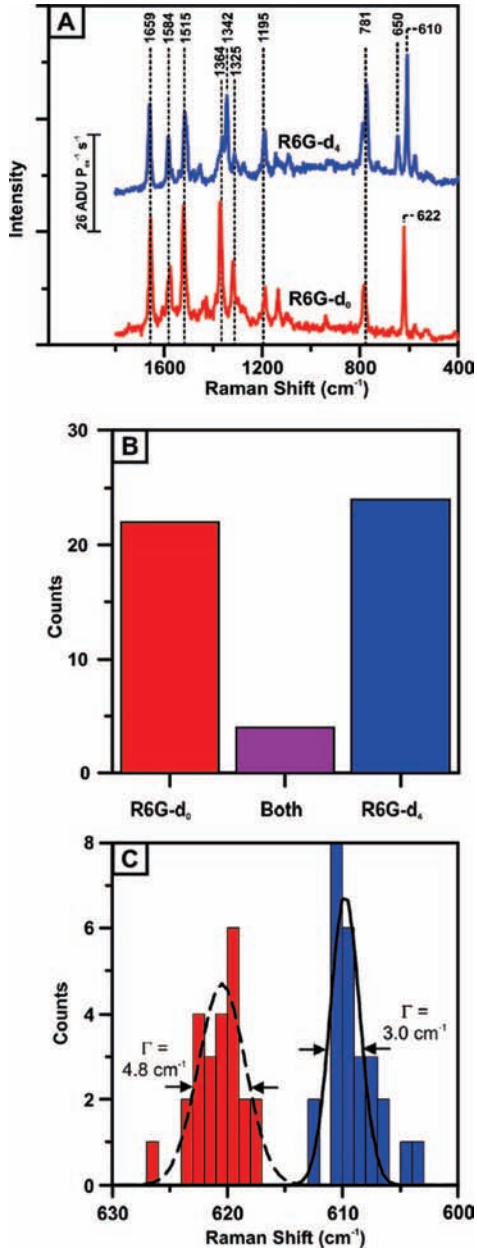

FIGURE 4. (A) Two representative spectra from the single-molecule results where one contains uniquely R6G-d_0 (red line) and the other uniquely R6G-d_4 (blue line) vibrational character. (λ_{ex} = 532 nm, t_{aq} = 10 s, P_{ex} = 2.4 W/cm^2, grazing incidence), (B) histogram detailing the frequency with which only R6G-d_0, only R6G-d_4, and both R6G-d_0 and R6G-d_4 vibrational modes were observed with low adsorbate concentration under dry N_2 environment, and (C) histogram of the low-frequency peak location for the events that exhibited single-molecule behavior, illustrating the degree of spectral changes observed for different sites. For R6G-d_0 (red data), the fwhm of the Gaussian fit was 4.8 cm^{-1}, and for R6G-d_4 (blue data), the fwhm of the Gaussian fit was 3.0 cm^{-1}. Reproduced with permission from ref 47. Copyright 2007 American Chemical Society.

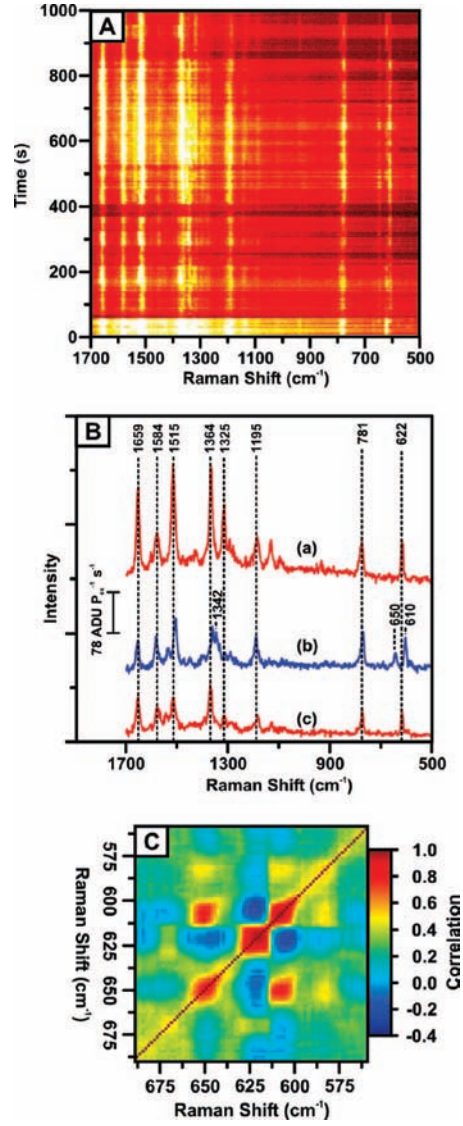

FIGURE 5. (A) Time series waterfall plot of spectra collected from a single active aggregate at high concentration in humid air with the false color representing signal intensity where white or yellow is highest and red or black is lowest, (B) three time slices from the waterfall plot shown in panel A where (a) = 51 s, (b) = 463 s, and (c) = 936 s showing that the system changes state from R6G-d_0 to R6G-d_4 and back in 1000 s (λ_{ex} = 532 nm, t_{aq} = 1 s, P_{ex} = 2.4 W/cm^2, grazing incidence), and (C) zero time delay two-dimensional cross-correlation of the time evolution data from panel A. Reproduced with permission from ref 47. Copyright 2007 American Chemical Society.

molecules are acting independently at two different hot spots within the probe area. In an effort to distinguish which case is taking place, the data were analyzed with 2D cross correlation.[49] If there are independent hot spots in close proximity, then the time evolution of the two molecules should be noncorrelated (χ = 0), but if it is the same hot spot, the molecules should be anticorrelated (χ= −1). Figure 5c shows the 2D correlation in the region containing the characteristic 650 and 610 cm^{-1} bands of the R6G-d_4 isotopologue. The spectra show strong correlation (χ = 0.8) between these two bands associated with R6G-d_4 and further show an anticorrelation (χ

$= -0.3$) from bands associated with the cross-peaks between R6G-d_0 and R6G-d_4. In SERS, there is an intense, continuous background that covers the entire spectral region of interest, and Moore et al.[50] have shown that in this 2D cross-correlation analysis, there will be strong correlation of the Stokes bands to this continuum. Therefore, even in the absence of a peak, there will be some time-correlated background contribution, which will affect the peak-to-peak correlation. This is evident in the ($\chi = 0.2-0.4$) correlation remaining between the background and the characteristic modes. This argues that the magnitude of the anticorrelation is larger, and therefore there is only one active hot spot in the probe volume, and molecules are moving in short-range proximity to it.

D. Enhancement Factors in Single-Molecule Surface-Enhanced Raman Scattering of Rhoadmine 6G. The original estimates of SMSERS enhancement factors ($\sim 10^{14}-10^{15}$)[3,4] are too large because those estimates did not take into account the large resonance Raman cross section of R6G.[51] To date, all the SMSERS studies of R6G were carried out at laser excitation wavelengths near the R6G molecular resonance and enhancement from the resonance Raman effect can contribute an additional factor of 10^2-10^3 in Raman scattering intensity compared with normal Raman.[52] Furthermore, the Raman cross section of R6G at 633 nm was measured to be 2.4×10^{-27} cm^2/sr,[51] and calculations on resonance[53,54] suggest values $\sim 10^{-25}$ cm^2. If the observed cross section is a simple multiplication of the R6G resonance Raman cross section and the SERS enhancement factor, the cross section observed by Nie and Emory (10^{-15} cm^2) requires a total SERS enhancement factor of only $10^{10}-10^{11}$. It is currently believed that a large part of this SMSERS enhancement can be attributed to the EM mechanism with the enhanced local fields at the junction of nanoparticle aggregates giving rise to EM enhancement factors of $10^{10}-10^{11}$.[55] Therefore, the SMSERS phenemonon results from multiplication of the combination of surface plasmon excitation and resonance Raman enhancement.

Another possible enhancement mechanism is a chemical or charge transfer (CT) mechanism that is caused by the changes in the electronic structure of molecules adsorbed on the metal surfaces. The role of metal to molecule charge transfer (CT) in SMSERS of R6G is not well understood. Since R6G SMSERS measurements were carried out on Ag nanoparticles, it is important to examine whether the absorption of R6G changes on a Ag surface.[56] Figure 6 shows the absorption spectrum of a submonolayer of R6G adsorbed on a Ag film. A major absorption band at 534 nm is observed in the spectrum. Compared with the R6G solution absorption, the major absorption band is red-shifted by only 2 nm and slightly broadened. These measurements show that R6G electronic transitions are, surprisingly, not significantly perturbed by the presence of the Ag surface.

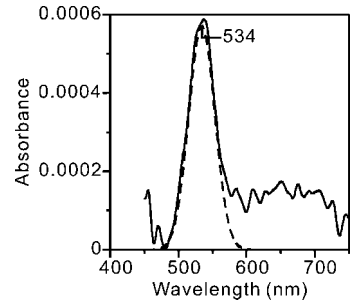

FIGURE 6. Absorption spectrum of R6G on a Ag film. Solid line represents the measured spectrum. Dashed line repents the Gaussian fitting of the spectrum. Reproduced from ref 56. Copyright 2007 American Chemical Society.

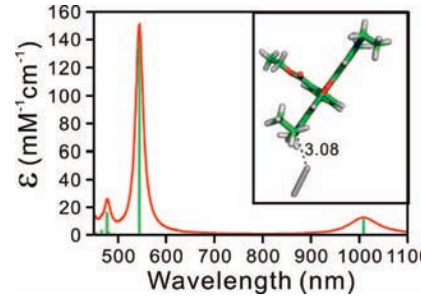

FIGURE 7. Calculated absorption spectrum of R6G with a Ag_2 cluster. Inset is the optimized structure of R6G$-Ag_2$. The distance between the N atom of R6G and the Ag atom is 3.08 Å. Reproduced from ref 56. Copyright 2007 American Chemical Society.

To examine whether new transitions from metal to molecule charge transfer arise when R6G adsorbs on a metallic surface from a theory perspective, we calculated the absorption spectrum of R6G interacting with a Ag_2 cluster with time-dependent density functional theory (TD-DFT).[56] The Ag_2 is used to represent R6G adsorption to Ag nanoparticles through one of its N atoms.[52,53] The calculated structure and absorption spectrum are shown in Figure 7. R6G with the Ag_2 cluster has a S_0-S_1 transition at 544 nm corresponding to an excitation from the highest occupied molecular orbital (HOMO) to the lowest unoccupied molecular orbital (LUMO). Two CT transitions red of the main peak are found at 1010 and 617 nm, corresponding to transitions from the HOMO of Ag_2 to the LUMO and LUMO + 1 of R6G, respectively. Both transitions have small oscillator strength, especially the transition at 617 nm, which is not visible in Figure 7 due to the *y* axis scale. These very weak CT transitions near 1000 nm will only affect the Raman scattering intensity when performed at these wavelengths, such as in FT-Raman. Therefore, when SMSERS is per-

formed at 532 nm, we conclude that the enhancement factor does not contain a contribution from CT.

IV. Concluding Remarks

The renewed interest in SERS has been driven by the ability to make reproducible and well-defined substrates with large electromagnetic enhancements and the discovery of single-molecule SERS. The recent developments, of which we highlight a few from work in our group, make the application of SERS to a range of problems in chemical and biological sensing a real possibility. Due to these strides, we believe the future of SERS is indeed bright.

This work was supported by the National Science Foundation (Grants CHE-0414554, DMR-0520513, EEC-0647560), the Air Force Office of Scientific Research (MURI Grant F49620-02-1-0381), the DTRA JSTO Program (Grant FA9550-06-1-0558), and DOE Grant DE-FG02-03ER15457. We gratefully acknowledge Dr. Lasse Jensen and Prof. George C. Schatz for the TD-DFT calculations presented in Figures 6 and 7. In addition, we thank present and former members of the Van Duyne group that have contributed so much to our SERS research effort including Lisa Dick, Christy Haynes, John Hulteen, Olga Lyandres, Adam McFarland, Nilam Shah, Paul Stiles, Douglas Stuart, David Treichel, Matthew Young, and Xiaoyu Zhang.

BIOGRAPHICAL INFORMATION

Jon P. Camden is currently Assistant Professor of Chemistry at the University of Tennessee, Knoxville. He received his B.S. in chemistry and music from the University of Notre Dame and his Ph.D. from Stanford University, where his work in the laboratory of Richard Zare was supported by a NSF Graduate Research Fellowship. He then completed postdoctoral research at Northwestern University with George Schatz and Richard Van Duyne. His research interests include surface-enhanced Raman scattering, modeling nanoparticle optical properties, and chemical reaction dynamics.

Jon A. Dieringer was born in Delphos, OH. He received his B.S. in chemistry at The Ohio State University in Columbus, OH, while performing research with Richard McCreery. He is currently a Ph.D. candidate in chemistry at Northwestern University. Richard Van Duyne is his research advisor. His research focuses on understanding single-molecule surface-enhanced Raman spectroscopy and extending it to tip-enhanced systems.

Jing Zhao received a B.S. in chemical physics from University of Science and Technology of China in 2003 and a Ph.D. from Northwestern University in 2008 where she worked with Richard Van Duyne and George Schatz. Her research focuses on the optical properties of nanoparticles and their interaction with resonant molecules.

Richard P. Van Duyne is Charles E. and Emma H. Morrison Professor of Chemistry at Northwestern University. He received his Ph.D. from the University of North Carolina at Chapel Hill. His research interests include surface-enhanced Raman spectroscopy, nanosphere lithography, localized surface plasmon resonance spectroscopy, molecular plasmonics, chemical and biological sensing, structure and function of biomolecules on surfaces, tip-enhanced Raman spectroscopy, ultrahigh vacuum scanning tunneling microscopy, ultrahigh vacuum surface science, Raman spectroscopy of mass-selected clusters, and application of surface-enhanced Raman spectroscopy to the study of works of art.

FOOTNOTES

* Corresponding author. E-mail: vanduyne@northwestern.edu.

REFERENCES

1 Jeanmarie, D. L.; Van Duyne, R. P. Surface Raman spectroelectrochemistry, Part 1: Heterocyclic, aromatic, and aliphatic amines adsorbed on the anodized silver electrode. *J. Electroanal. Chem.* **1977**, *84*, 1–20.

2 Albrecht, M. G.; Creighton, J. A. Anomalously intense Raman spectra of pyridine at a silver electrode. *J. Am. Chem. Soc.* **1977**, *99*, 5215–5217.

3 Nie, S.; Emory, S. R. Probing single molecules and single nanoparticles by surface-enhanced Raman scattering. *Science* **1997**, *275*, 1102–1106.

4 Kneipp, K.; Wang, Y.; Kneipp, H.; Perelman, L. T.; Itzkan, I.; Dasari, R. R.; Feld, M. S. Single molecule detection using surface-enhanced Raman scattering (SERS). *Phys. Rev. Lett.* **1997**, *78*, 1667–1670.

5 Haynes, C. L.; Yonzon, C. R.; Zhang, X. Y.; Van Duyne, R. P. Surface-enhanced Raman sensors: early history and the development of sensors for quantitative biowarfare agent and glucose detection. *J. Raman Spectrosc.* **2005**, *36*, 471–484.

6 Moskovits, M. Surface-enhanced Raman spectroscopy: a brief retrospective. *J. Raman Spectrosc.* **2005**, *36*, 485–496.

7 Moskovits, M. Surface-enhanced spectroscopy. *Rev. Mod. Phys.* **1985**, *57*, 783–826.

8 Otto, A.; Mrozek, I.; Grabhorn, H.; Akemann, W. Surface-enhanced Raman-scattering. *J. Phys.: Condens. Matter* **1992**, *4*, 1143–1212.

9 Campion, A.; Kambhampati, P. Surface-enhanced Raman scattering. *Chem. Soc. Rev.* **1998**, *27*, 241–250.

10 Stiles, P. L.; Dieringer, J. A.; Shah, N. C.; Van Duyne, R. P. Surface-enhanced Raman spectroscopy. *Annu. Rev. Anal. Chem.* **2008**, in press.

11 Jensen, T. R.; Malinsky, M. D.; Haynes, C. L.; Van Duyne, R. P. Nanosphere lithography: Tunable localized surface plasmon resonance spectra of silver nanoparticles. *J. Phys. Chem. B* **2000**, *104*, 10549–10556.

12 Haynes, C. L.; Van Duyne, R. P. Nanosphere lithography: A versatile nanofabrication tool for studies of size-dependent nanoparticle optics. *J. Phys. Chem. B* **2001**, *105*, 5599–5611.

13 Haynes, C. L.; Van Duyne, R. P. Plasmon-sampled surface-enhanced Raman excitation spectroscopy. *J. Phys. Chem. B* **2003**, *107*, 7426–7433.

14 Haes, A. J.; Zou, S. L.; Schatz, G. C.; Van Duyne, R. P. A nanoscale optical biosensor: The long range distance dependence of the localized surface plasmon resonance of noble metal nanoparticles. *J. Phys. Chem. B* **2004**, *108*, 109–116.

15 McFarland, A. D.; Young, M. A.; Dieringer, J. A.; Van Duyne, R. P. Wavelength-scanned surface-enhanced Raman excitation spectroscopy. *J. Phys. Chem. B* **2005**, *109*, 11279–11285.

16 Dick, L. A.; McFarland, A. D.; Haynes, C. L.; Van Duyne, R. P. Metal film over nanosphere (MFON) electrodes for surface-enhanced Raman spectroscopy (SERS): Improvements in surface nanostructure stability and suppression of irreversible loss. *J. Phys. Chem. B* **2002**, *106*, 853–860.

17 Lyandres, O.; Shah, N. C.; Yonzon, C. R.; Walsh, J. T.; Glucksberg, M. R.; Van Duyne, R. P. Real-time glucose sensing by surface-enhanced Raman Spectroscopy in bovine plasma facilitated by a mixed decanethiol/mercaptohexanol partition layer. *Anal. Chem.* **2005**, *77*, 6134–6139.

18 Stuart, D. A.; Yonzon, C. R.; Zhang, X. Y.; Lyandres, O.; Shah, N. C.; Glucksberg, M. R.; Walsh, J. T.; Van Duyne, R. P. Glucose sensing using near-infrared surface-enhanced Raman spectroscopy: Gold surfaces, 10-day stability, and improved accuracy. *Anal. Chem.* **2005**, *77*, 4013–4019.

19 Shah, N. C.; Lyandres, O.; Walsh, J. T.; Glucksberg, M. R.; Van Duyne, R. P. Lactate and sequential lactate-glucose sensing using surface-enhanced Raman spectroscopy. *Anal. Chem.* **2007**, *79*, 6927–6932.

20 Stuart, D. A.; Yuen, J. M.; Shah, N. C.; Lyandres, O.; Yonzon, C. R.; Glucksberg, M. R.; Walsh, J. T.; Van Duyne, R. P. In vivo glucose measurement by surface-enhanced Raman spectroscopy. *Anal. Chem.* **2006**, *78*, 7211–7215.

21 Zhang, X.; Young, M. A.; Lyandres, O.; Van Duyne, R. P. Rapid detection of an anthrax biomarker by surface-enhanced Raman spectroscopy. *J. Am. Chem. Soc.* **2005**, *127*, 4484–4489.

22 Zhang, X.; Zhao, J.; Whitney, A.; Elam, J.; Van Duyne, R. P. Ultrastable substrates for surface-enhanced Raman spectroscopy fabricated by atomic layer deposition: Improved anthrax biomarker detection. *J. Am. Chem. Soc.* **2006**, *128*, 10304–10309.

23 Hicks, E. M.; Zhang, X. Y.; Zou, S. L.; Lyandres, O.; Spears, K. G.; Schatz, G. C.; Van Duyne, R. P. Plasmonic properties of film over nanowell surfaces fabricated by nanosphere lithography. *J. Phys. Chem. B* **2005**, *109*, 22351–22358.

24 Whitney, A. V.; Elam, J. W.; Zou, S. L.; Zinovev, A. V.; Stair, P. C.; Schatz, G. C.; Van Duyne, R. P. Localized surface plasmon resonance nanosensor: A high-resolution distance-dependence study using atomic layer deposition. *J. Phys. Chem. B* **2005**, *109*, 20522–20528.

25 Yonzon, C. R.; Zhang, X.; Zhao, J.; Van Duyne, R. P. Surface-enhanced nanosensors. *Spectroscopy* **2007**, *22*, 42.

26 Kerker, M.; Wang, D. S.; Chew, H. Surface Enhanced Raman-Scattering (Sers) by Molecules Adsorbed at Spherical-Particles. *Appl. Opt.* **1980**, *19*, 4159–4174.

27 Gersten, J.; Nitzan, A. Electromagnetic Theory of Enhanced Raman-Scattering by Molecules Adsorbed on Rough Surfaces. *J. Chem. Phys.* **1980**, *73*, 3023–3037.

28 Metiu, H.; Das, P. The electromagnetic theory of surface enhanced spectroscopy. *Annu. Rev. Phys. Chem.* **1984**, *35*, 507–536.

29 Schatz G. C.; Van Duyne, R. P. In *Handbook of Vibrational Spectroscopy*; Chalmers, J. M., Griffiths, P. R., Eds.; John Wiley & Sons Ltd.: New York, 2002; pp 759−774.

30 Blatchford, C. G.; Campbell, J. R.; Creighton, J. A. Plasma resonance enhanced Raman-scattering by adsorbates on gold colloids - the effects of aggregation. *Surf. Sci.* **1982**, *120*, 435–455.

31 Vlckova, B.; Gu, X. J.; Moskovits, M. SERS excitation profiles of phthalazine adsorbed on single colloidal silver aggregates as a function of cluster size. *J. Phys. Chem. B* **1997**, *101*, 1588–1593.

32 Felidj, N.; Aubard, J.; Levi, G.; Krenn, J. R.; Hohenau, A.; Schider, G.; Leitner, A.; Aussenegg, F. R. Optimized surface-enhanced Raman scattering on gold nanoparticle arrays. *Appl. Phys. Lett.* **2003**, *82*, 3095–3097.

33 Dick, L. A.; Haes, A. J.; Van Duyne, R. P. Distance and orientation dependence of heterogeneous electron transfer: A surface-enhanced resonance Raman scattering study of cytochrome c bound to carboxylic acid terminated alkanethiols adsorbed on silver electrodes. *J. Phys. Chem. B* **2000**, *104*, 11752–11762.

34 Kennedy, B. J.; Spaeth, S.; Dickey, M.; Carron, K. T. Determination of the distance dependence and experimental effects for modified SERS substrates based on self-assembled monolayers formed using alkanethiols. *J. Phys. Chem. B* **1999**, *103*, 3640–3646.

35 Dieringer, J. A.; McFarland, A. D.; Shah, N. C.; Stuart, D. A.; Whitney, A. V.; Yonzon, C. R.; Young, M. A.; Zhang, X.; Van Duyne, R. P. Surface enhanced Raman spectroscopy: New materials, concepts, characterization tools, and applications. *Faraday Discuss.* **2005**, *132*, 9–26.

36 Kneipp, K.; Kneipp, H.; Bohr, H. G. In *Surface-Enhanced Raman Scattering: Physics and Applications*; Kneipp, K., Moskovits, M., Kneipp, H., Eds.; Topics in Applied Physics, Vol. 103; Springer: Berlin, 2006; pp 261−277.

37 Andersen, P. C.; Jacobson, M. L.; Rowlen, K. L. Flashy silver nanoparticles. *J. Phys. Chem. B* **2004**, *108*, 2148–2153.

38 Domke, K. F.; Zhang, D.; Pettinger, B. Enhanced Raman spectroscopy: Single molecules or carbon. *J. Phys. Chem. C* **2007**, *111*, 8611–8616.

39 Etchegoin, P. G.; Meyer, M.; Le Ru, E. C. Statistics of single molecule SERS signals: Is there a Poisson distribution of intensities. *Phys. Chem. Chem. Phys.* **2007**, *9*, 3006–3010.

40 Doering, W. E.; Nie, S. M. Single-molecule and single-nanoparticle SERS: Examining the roles of surface active sites and chemical enhancement. *J. Phys. Chem. B* **2002**, *106*, 311–317.

41 Michaels, A. M.; Nirmal, M.; Brus, L. E. Surface enhanced Raman spectroscopy of individual rhodamine 6G molecules on large Ag nanocrystals. *J. Am. Chem. Soc.* **1999**, *121*, 9932–9939.

42 Michaels, A. M.; Jiang, J.; Brus, L. Ag nanocrystal junctions as the site for surface-enhanced Raman scattering of single rhodamine 6G molecules. *J. Phys. Chem. B* **2000**, *104*, 11965–11971.

43 Le Ru, E. C.; Meyer, M.; Etchegoin, P. G. Proof of single-molecule sensitivity in surface enhanced Raman scattering (SERS) by means of a two-analyte technique. *J. Phys. Chem. B* **2006**, *110*, 1944–1948.

44 Etchegoin, P. G.; Meyer, M.; Blackie, E.; LeRu, E. C. Statistics of single-molecule surface enhanced Raman scattering signals: Fluctuation analysis with multiple analyte techniques. *Anal. Chem.* **2007**, *79*, 8411–8415.

45 Goulet, P. J. G.; Aroca, R. F. Distinguishing individual vibrational fingerprints: Single-molecule surface-enhanced resonance Raman scattering from one-to-one binary mixtures in Langmuir−Blodgett monolayers. *Anal. Chem.* **2007**, *79*, 2728–2734.

46 Sawai, Y.; Takimoto, B.; Nabika, H.; Ajito, K.; Murakoshi, K. Observation of a small number of molecules at a metal nanogap arrayed on a solid surface using surface-enhanced Raman scattering. *J. Am. Chem. Soc.* **2007**, *129*, 1658–1662.

47 Dieringer, J. A.; Lettan, R. B., II; Scheidt, K. A.; Van Duyne, R. P. A frequency domain existence proof of single-molecule surface-enhanced Raman spectroscopy. *J. Am. Chem. Soc.* **2007**, *129*, 16249–16256.

48 Kneipp, K.; Kneipp, H.; Itzkan, I.; Dasari, R. R.; Feld, M. S. Surface-enhanced Raman scattering: A new tool for biomedical spectroscopy. *Curr. Sci.* **1999**, *77*, 915–924.

49 Noda, I.; Ozaki, Y. *Two-Dimensional Correlation Spectroscopy - Applications in Vibrational and Optical Spectroscopy*; John Wiley and Sons, Ltd.: Chichester, West Sussex, U.K., 2004.

50 Moore, A. A.; Jacobson, M. L.; Belabas, N.; Rowlen, K. L.; Jonas, D. M. 2D correlation analysis of the continuum in single molecule surface enhanced Raman spectroscopy. *J. Am. Chem. Soc.* **2005**, *127*, 7292–7293.

51 Le Ru, E. C.; Blackie, E.; Meyer, M.; Etchegoin, P. G. Surface enhanced Raman scattering enhancement factors: A comprehensive study. *J. Phys. Chem. C* **2007**, *111*, 13794–13803.

52 Hildebrandt, P.; Stockburger, M. Surface-enhanced resonance Raman-spectroscopy of rhodamine-6g adsorbed on colloidal silver. *J. Phys. Chem.* **1984**, *88*, 5935–5944.

53 Watanabe, H.; Hayazawa, N.; Inouye, Y.; Kawata, S. DFT vibrational calculations of rhodamine 6G adsorbed on silver: Analysis of tip-enhanced Raman spectroscopy. *J. Phys. Chem. B* **2005**, *109*, 5012–5020.

54 Jensen, L.; Schatz, G. C. Resonance Raman scattering of rhodamine 6G as calculated using time-dependent density functional theory. *J. Phys. Chem. A* **2006**, *110*, 5973–5977.

55 Xu, H. X.; Aizpurua, J.; Kall, M.; Apell, P. Electromagnetic contributions to single-molecule sensitivity in surface-enhanced Raman scattering. *Phys. Rev. E* **2000**, *62*, 4318–4324.

56 Zhao, J.; Jensen, L.; Sung, J. H.; Zou, S. L.; Schatz, G. C.; Van Duyne, R. P. Interaction of plasmon and molecular resonances for rhodamine 6G adsorbed on silver nanoparticles. *J. Am. Chem. Soc.* **2007**, *129*, 7647–7656.